



2 North Atlantic geoid high, volcanism and glaciations

3 Eugenio Carminati^{1,2} and Carlo Doglioni^{1,2}

4 Received 4 November 2009; revised 15 December 2009; accepted 23 December 2009; published XX Month 2010.

6 [1] Shallow topography, geoid high and intense volcanism
7 in the northern Mid Atlantic Ridge are interpreted as
8 enhanced by the loading on the adjacent continents by ice
9 caps during upper Cenozoic glaciations. The load of ice
10 packs on the continental lithospheres of North America and
11 northern Europe generated radial mantle flow at depth. In
12 our model, these currents, flowing from west and east, faced
13 each other below the northern Atlantic, joining together and
14 upwelling. Numerical modeling of this process supports the
15 development of dynamic topography leading to uplift of the
16 sea-floor and inducing a regional geoid high. The mantle
17 rising to shallower levels may have contributed to larger
18 asthenospheric melting, and to ridge centered excess
19 magmatism, as observed in the Northern Atlantic.

20 **Citation:** Carminati, E., and C. Doglioni (2010), North
21 Atlantic geoid high, volcanism and glaciations, *Geophys. Res.*
22 *Let.*, 37, LXXXXX, doi:10.1029/2009GL041663.

24 1. Introduction

25 [2] The lithosphere generated by the Mid Atlantic Ridge
26 (MAR) east of Greenland underlies the youngest (<60 Myr)
27 and narrowest part of the Atlantic Ocean. This portion of the
28 northern Atlantic shows three peculiar characters, 1) it is
29 about 1–3 km shallower than the average mid-oceanic ridge
30 (Figures 1a and 1b); 2) it displays diffuse positive gravity
31 (>30 mGal) and geoid (>50 m) anomalies (Figures 1c, 1d,
32 and 1f); 3) it is the seat of larger than average magmatic
33 productivity, resulting in the thickest oceanic crust of the
34 entire MAR, up to about 40 km below Iceland [Kaban *et al.*,
35 2002]. The thickness of the Cretaceous-Early Cenozoic
36 (pre-glaciations) oceanic crust in the northern Atlantic is
37 rather 4–6 km in average [e.g., Shillington *et al.*, 2006].

38 [3] A number of papers attributed these features to the
39 Iceland mantle plume [Vink, 1984]. However, the deep
40 hotspot hypothesis has been questioned on various grounds
41 [e.g., Foulger and Anderson, 2005]: the persistence of
42 magmatism on the westerly moving ridge and the presence
43 of a double tail both west and east of Iceland; the absence of
44 a relevant heat flow positive anomaly, and the possible
45 presence of a hydrous mantle lowering the melting point
46 [Bonath, 1990; Asimow and Langmuir, 2003]. There is also
47 contrasting topologic and tomographic evidence on whether
48 the source of the plume is in the deep or in the upper mantle
49 [Foulger *et al.*, 2001; Courtillot *et al.*, 2003; Ritsema and
50 Allen, 2003; Montelli *et al.*, 2004]. Moreover, the geochem-
51 ical Icelandic signature is not restricted to Iceland, but
52 continues both north and south along the Mid Atlantic

Ridge [Taylor *et al.*, 1997]. In this article we test numeri- 53
cally a model in which the far field superficial loading of the 54
mantle by the ice caps in North America and northern 55
Europe can contribute to generate the anomalous features 56
of the North Atlantic. 57

[4] Jull and McKenzie [1996] and MacLennan *et al.* 58
[2002] have demonstrated that the removal of ice load over 59
Iceland triggers volcanism. Here we show that an inverse 60
correlation can occur for magma production, i.e., the ice 61
loading on the adjacent continental areas may have contrib- 62
uted to the uplift of the north Atlantic mantle, to the geoid 63
anomaly and, possibly, to the higher degree of melting 64
due to faster adiabatic decompression induced by mantle 65
upwelling. 66

2. Model Description and Results

[5] Assuming a viscous Earth (uniform viscous half- 68
space) and a cylindrical ice-load, it can be shown by 69
analytical solutions [e.g., Cathles, 1975] that the depth at 70
which the vertical displacement induced by ice loading/ 71
unloading is 0.5, 0.2 or 0.1 times the surface value is equal 72
to $1.4R_0$, $2.5R_0$ and $3.3R_0$ (where R_0 is the radius of the 73
cylinder; i.e., 825 km, 1474 km and 1815 km for the 74
Fennoscandian ice sheet, characterized by $R_0 = 550$ km) 75
respectively. Numerical solutions have also shown that the 76
ice cycles in the Canadian region induced vertical motions 77
(either uplift or subsidence) up to more than 60° (more than 78
6600 km) from the ice center [e.g., Cathles, 1975]. 79

[6] Here we test the combined effects the glacial cycles in 80
North America and Europe on regional mantle flow. The 81
aim of our finite element modeling, performed using COM- 82
SOL 3.5 software (<http://www.comsol.com/>), is to evaluate 83
the velocity field induced within the upper mantle by 84
glaciation cycles rather than to reproduce exactly the surface 85
velocities. This limited objective allowed us to adopt some 86
major simplifying assumptions, such as the 2D nature of the 87
model, neglecting the load due to water redistribution 88
during the ice formation and melting, and using a simplified 89
ice model. 90

[7] The model adopts a 2D plane strain approximation 91
and includes lithosphere, upper and lower mantle (Figure 2). 92
All the layers are described by a compressible linear 93
viscoelastic (Maxwell) rheology; the assumed elastic con- 94
stants and viscosities are listed in Table 1. The elastic 95
structure is consistent with the PREM model [Dziewonski 96
and Anderson, 1981] and the viscosities are consistent with 97
values normally used for glacial isostatic rebound modeling 98
[e.g., Mitrovica and Peltier, 1993; Kaufmann and Lambeck, 99
2002]. Gravity acceleration and density vary with depth 100
according to the PREM model. Gravity is applied as a body 101
force and the ice load as a boundary condition. The ice 102
thickness varies with time but it is kept laterally constant for 103
each area. The model is run from 150 Kyr BP to the present. 104

¹Dipartimento di Scienze della Terra, Università di Roma “La Sapienza,” Rome, Italy.

²Istituto Geologia Ambientale e Geoingegneria, CNR, Rome, Italy.

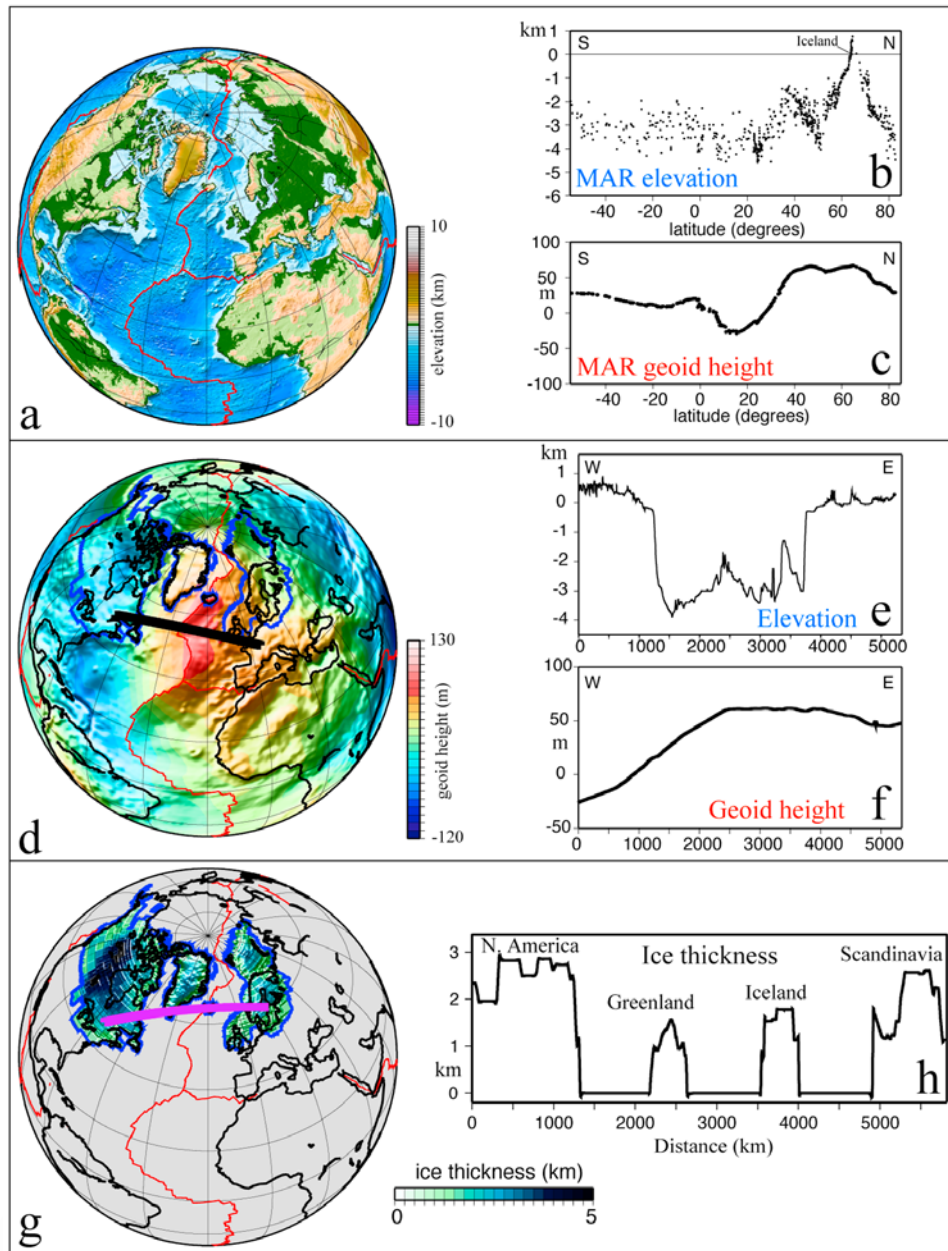


Figure 1. (a) Topography (data after ETOPO1, <http://www.ngdc.noaa.gov/mgg/global/global.html>); (b) elevation of the Mid Atlantic Ridge; the bathymetric distribution along the MAR shows a high in the northern Atlantic which is limited not only to the Iceland area but it extends ca 20° northward and 40° southward; (c) geoid anomaly along the Mid Atlantic Ridge (data after the EGM96 model, <http://cddis.nasa.gov/926/egm96/egm96.html>); (d) geoid height; notice how the northern Atlantic geoid high is located between the North American and Scandinavian ice bodies; (e) topography-bathymetry along the cross-section on the map to the left; (f) geoid height along the same section. The blue curves in panel Figure 1d show the borders of the ice bodies according to ICE-5G. The geoid is shallower along the eastern flank of MAR and the crest of the anomaly is offset to the east of the oceanic ridge. (g) Thickness in map and (h) cross-section in purple of the ice cap at the last glacial maximum (21 Kyr BP; data after the ICE-5G model [Peltier, 2004]). Mid-ocean ridges are shown as red lines. The purple great circle in Figure 1g shows the trace of the modeled profile of Figure 2.

105 The ice thickness is kept at zero between 150 Kyr and
 106 120 Kyr BP and then it is linearly increased to reach the
 107 maximum thickness at 105 Kyr BP. It is then kept constant
 108 until 21 Kyr BP. Between 21 Kyr and 6 Kyr BP the ice
 109 thickness is linearly decreased to zero, with the exception of
 110 Greenland, where it is decreased to 750 m. The maximum
 111 thicknesses is assumed to vary regionally: 2500 m for North

America, 1300 m for Greenland, 2000 m for Scandinavia
 112 and 2000 m for Iceland (when applied). Such values are
 113 consistent with the diagram of Figure 1h, showing maxi-
 114 mum ice thicknesses along the trace of the modeled section
 115 at 21 Kyr BP according to the ICE-5G model [Peltier,
 116 2004]. The bottom of the model is fixed normally to the
 117 boundary and free to slip tangentially. Symmetry conditions
 118

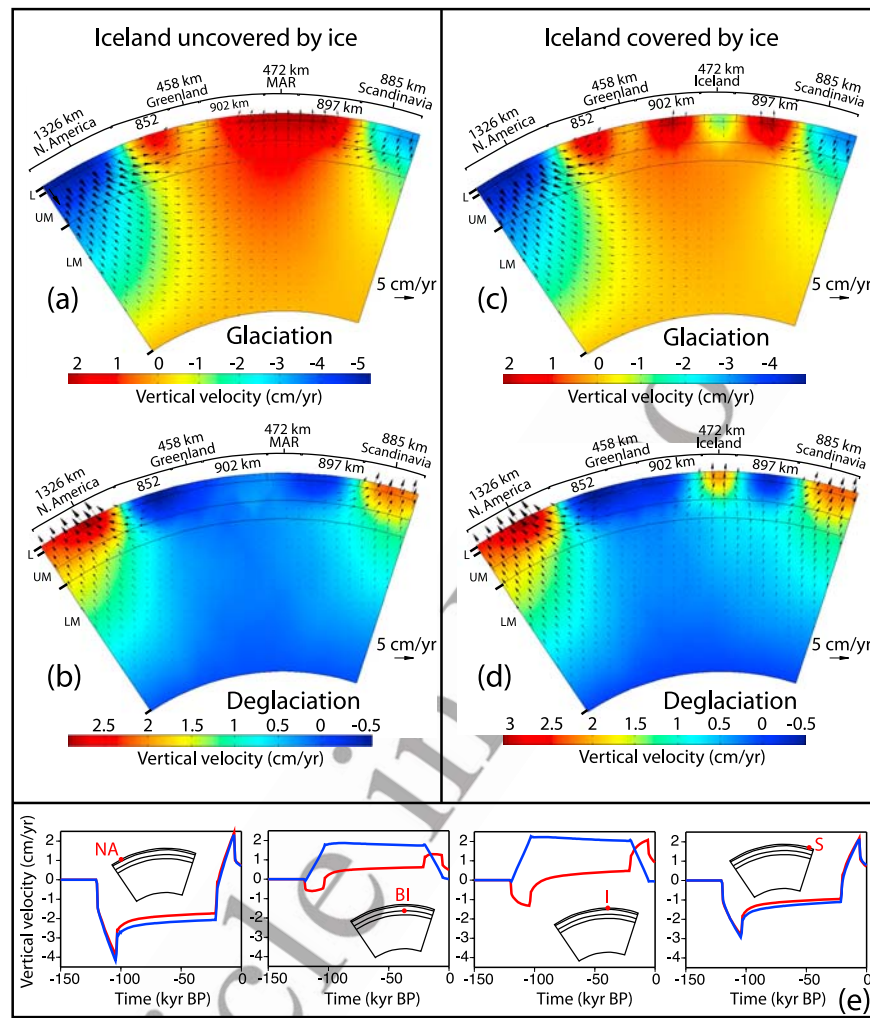


Figure 2. Vertical velocities and velocity fields predicted by the models (a and c) immediately after the formation of the ice caps (105 Kyr BP) and (b and d) soon after their melting (6 Kyr BP). Figures 2a and 2b are referred to a model characterized by the absence of ice during the glacial period in the Iceland region, while panels c and d to a model characterized by Iceland affected by ice. (e) Vertical rates through time at four different locations marked by the red dots (NA, North America; BI, beneath Iceland; I, Iceland; S, Scandinavia). Blue line is with Iceland unaffected by ice, whereas the red line represents the case of Iceland covered by ice.

119 are imposed on the left and right boundaries. This is
 120 reasonable since the tips of the modeled section are located
 121 approximately at the center of the American and Scandina-
 122 vian ice masses. The model surface is left free in areas
 123 unaffected by ice formation. We use a set of ca. 3800
 124 triangular elements. Modeling results are shown for the
 125 time steps of 105 Kyr and 6 Kyr BP, representative of the
 126 glaciation and deglaciation scenarios respectively. Although
 127 no constraints are available for past mantle velocity simu-
 128 lations, we are confident that the patterns and the order of
 129 magnitude of the calculated velocities are realistic. This
 130 confidence is justified by the positive match between
 131 simulated and observed present-day vertical velocities for
 132 well-constrained areas such as Scandinavia.

133 [8] Two scenarios are modeled. In the first Iceland is
 134 covered by ice during the glaciation, while in a second
 135 Iceland is assumed to be ice-free. The first model simulates
 136 the evolution in the transect of Figure 1, while the second
 137 simulates a section just north or south of Iceland. Figure 2
 138 shows the vertical velocities and the velocity field predicted

for the two scenarios. Both scenarios indicate a convergence
 of velocity vectors towards the Atlantic area during forma-
 tion of the ice cap, with a prevalence of horizontal directions
 of motion. Below Iceland and the surrounding Atlantic the
 velocity vectors turn vertical with a general upwelling (rates
 of up to 2 cm/yr in the Iceland ice-free scenario). In the
 Iceland-covered scenario, the upwelling is limited to the
 Atlantic region with rates of less than 2 cm/yr. Below
 Iceland the lowermost upper mantle moves upward at slow
 rates (<0.5 cm), while the shallower upper mantle moves
 downward, due to the Icelandic ice load. During the same
 glaciation period, a negative (i.e., downward) velocity field
 with rates of $-2/-4$ cm/yr is predicted for North America
 and Scandinavia.

[9] The velocity field is reversed during deglaciation, with
 the mantle flowing downward and away from the central
 Atlantic region and upward below Scandinavia and North
 America. Figure 2e shows that the development of the
 velocity field associated to glaciation and its reversal
 during deglaciation is very fast, due to the elastic compo-

t1.1 **Table 1.** Elastic and Viscous Parameters Used in the Calculations

t1.2 Layer	Poisson's Ratio	Young Modulus (Pa)	Viscosity (Pa s)	Depth Interval (km)
t1.3 Lithosphere	0.27	1.75e11	5e22	0–100
t1.4 Upper Mantle	0.27	1.39e11	1e21	100–670
t1.5 Lower Mantle	0.27	1.27e11	1e22	670–2890

159 nent of rheology. Present-day rates, although with lower
 160 magnitude, show for the two scenarios velocity patterns
 161 similar to those of Figures 2b and 2d. This is consistent with
 162 literature [e.g., *Vestøl, 2006; Milne et al., 2001*]. Thus the
 163 dynamic topography attained during the glaciation period
 164 has not been completely recovered, due to the viscous
 165 component of the rheology of lithosphere and mantle.
 166 Although not shown, a sensitivity analysis showed that
 167 the described patterns of the velocity field are stable also
 168 when the rheological parameters and ice thickness are
 169 modified within reasonable bounds.

170 [10] Therefore the models show that the ice load induces
 171 a upward flow below the Mid Atlantic ridge generating a
 172 dynamic topography consistent with the geoid high mea-
 173 sured in the region. The results of the model that assumes
 174 Iceland free of ice allowed us to predict, at 21 ka BP (i.e.,
 175 just before the beginning of deglaciation), a geoid anomaly
 176 of ca. 70 m for the center of the Atlantic ocean (location I in
 177 Figure 2e). The geoid anomaly was calculated as $\Delta h =$
 178 $-\frac{2\pi G}{g} \int \Delta \rho(z) z dz$ [*Turcotte and Schubert, 2002*], where
 179 Δh is the geoid anomaly, g is the gravity acceleration,
 180 $\Delta \rho(z)$ is the anomalous density at depth z and D is the
 181 compensation depth (chosen as the bottom of our model) and
 182 G is the Newtonian constant ($6.67 \times 10^{11} \text{ m}^3 \text{ kg}^{-1} \text{ m}^{-2}$).
 183 Although this calculation is to be considered a rough
 184 estimate, since it includes only the upward motion of
 185 particles below the MAR and does not include crust
 186 formation, mantle partial melting and other thermal pro-
 187 cesses, it is compatible with the present day anomaly of the
 188 region (ca. 60 m; Figure 1), showing that present-day geoid
 189 anomaly and high topography of the region are remnants of
 190 the glaciation. These findings also explain the topographic
 191 low below Scandinavia and North America, consistent with
 192 the observed geoid low (the low geoid anomaly of North
 193 America has been already tentatively explained with the ice
 194 load by *Turcotte and Schubert [2002]*).

195 [11] Moreover, mantle upwelling may enhance mantle
 196 partial melting and explain, at least in part, the anomalously
 197 intense magmatic activity of the region. Assuming an
 198 average 7–10% melt of the asthenosphere [e.g., *Langmuir*
 199 *and Forsyth, 2007*] under the northern Mid Atlantic Ridge,
 200 the cumulative uplift of ca. 2 km of the mantle during the
 201 glaciations would increase the melting by a few percent
 202 (depending on water content, initial mantle composition and
 203 temperature, spreading rate, etc.), producing a larger volume
 204 of magma delivered to the surface.

205 3. Discussion and Conclusions

206 [12] Our modeling has shown, consistently with previous
 207 studies, that ice loading/unloading can have a regional
 208 impact on mantle flow velocities. The MAR swollen
 209 bathymetry (Figure 1) and the geoid regional positive
 210 anomaly of the northern Atlantic [*Lemoine et al., 1998;*
 211 *Tapley et al., 2005*] are located in an area intermediate

between the ice caps in Northern America and Europe 212
 during the last glaciation. Moreover, the same area is 213
 occupied by the largest volcanic province of the northern 214
 Atlantic. If our model is correct, we speculate a glacio- 215
 eustatic Milankovitch periodicity in north Atlantic magma 216
 production. 217

[13] The oldest rocks in Iceland are about 15 Ma old 218
 [*Hardarson et al., 1997*]. The same Authors noted chemical 219
 variations of basalts, generated by a variably depleted 220
 mantle. Iceland possibly emerged at that time or later, and 221
 it experienced ice loading as well. The time of the onset of 222
 glaciations in the northern hemisphere is still debated. It has 223
 been shown how the onset of glaciations in the northern 224
 hemisphere is older (Eocene-Oligocene) than previously 225
 estimated [*Eldrett et al., 2007*]. Recent deep sea drilling 226
 provided evidence for a middle Eocene initiation of the 227
 icehouse of the Arctic area [*Moran et al., 2006*]. High 228
 magma productivity has been documented in Iceland 13– 229
 11 Myr, and 8–7 Myr intervals together with periodicity in 230
 magma composition [e.g., *Kitagawa et al., 2008*]. *Gee et al.* 231
 [1998] detected a close relationship between the geochem- 232
 istry of lavas and glacioisostasy. They found that eruption 233
 of primitive lavas with depleted chemical and isotopic 234
 characteristics coincides with a period of glacioisostatic 235
 instability at the end of the last glaciation (13–9 Kyr). 236

[14] *Sigvaldason [2002]* described a Holocene rhyolitic 237
 eruption triggered by the melting of the ice cap in central- 238
 eastern Iceland, hinting at a relation between magmatic 239
 emplacement and vertical loading. 240

[15] Therefore, loading and unloading of the ice cap 241
 [*Watts, 2001*] appears to be a factor controlling locally or 242
 even regionally the production of mantle melts. Although 243
 we modeled a single ice cycle, the productivity of magma 244
 over geological periods is expected to be influenced by the 245
 superposition of several ice cycles on the process of oceanic 246
 spreading. The remote loading of ice can determine an 247
 upwelling of the mantle elsewhere, generating larger vol- 248
 umes of melt due to mantle adiabatic decompression below 249
 the ridge. Vice versa, the ice load in a volcanic area (e.g., 250
 along the MAR in Iceland) can locally buffer eruption, 251
 tuning the frequency of magmatic delivery, and generating a 252
 lower degree of melting and a longer residence time of 253
 melts in the mantle. These factors, together with the variable 254
 source depth of the melts, could cause significant variations 255
 of the lava's geochemistry. Therefore, in Iceland, the fol- 256
 lowing two complementary processes could interfere, over- 257
 lap, and buffer each other: deglaciation-induced magmatism 258
 (a in-situ mechanism associated with stress release related to 259
 ice unloading) and glaciation-induced magma production 260
 (a far-field effect, as shown by our model). In the remaining 261
 areas of the MAR, not directly covered by ice, a different 262
 time correlation between magma production and eruption is 263
 expected. 264

[16] Our model predicts a relatively low intensity of 265
 magmatism along the northern segment of the MAR during 266
 the present interglacial period. We note that the North 267
 Atlantic geoid height is presently decreasing, while it is 268
 increasing on the adjacent continental areas, as shown by 269
 the Grace project data [e.g., *Tapley et al., 2004*]. The 270
 decrease of the geoid has been related to the melting of 271
 ice in Greenland [*Ramillien et al., 2006*], but it could be 272
 related also to the decreasing upwelling beneath the north- 273

274 ern MAR due to the absence of ice caps on the continents.
 275 Conversely, the continental areas show an increase of the
 276 geoid because the mantle is rising, recovering the subsi-
 277 dence previously generated by the ice loading. However,
 278 when the mantle rises and melts beneath a ridge [McKenzie,
 279 1984], it becomes lighter [Oxburgh and Parmentier, 1977].
 280 Therefore the process is possibly not entirely reversible
 281 since the uplifted and depleted mantle cannot be re-pulled
 282 down at its original position, by the down-flow motion
 283 induced by deglaciation, because of the permanent increase
 284 in buoyancy characterizing the mantle after melting.

285 [17] During the time frame considered (e.g., say the last
 286 20–30 Ma) we may expect about 180–250 oscillations
 287 associated to the eccentricity of the Earth's orbit, or more
 288 than twice oscillations in case of obliquity related cycles.
 289 The model presented rather shows the effects of only one
 290 single cycle of loading and unloading. Assuming an irre-
 291 versible component on each cycle, the present geoid high
 292 would represent the sum of the all episodes, a sort of
 293 vibration generating hysteresis in the uplift of the mantle.

294 [18] In summary, we suggest that the ice caps on the
 295 continents of the northern hemisphere generated a flow in the
 296 underlying mantle that converges in the northern Atlantic
 297 from west and east, upwelling along the northern MAR. The
 298 eastward offset of the geoid high relative to the MAR could
 299 be due to a larger ice load on the northern American
 300 continent, although we cannot neglect a contribution from
 301 the relative eastward mantle flow implicit in the notion of
 302 the net rotation of the lithosphere [Gripp and Gordon,
 303 2002], able to generate an asymmetry of ocean ridges
 304 worldwide [Doglioni et al., 2003]. This model implies that
 305 the over production of magmatism in the northern Atlantic
 306 could be sourced by the shallower location of the astheno-
 307 sphere, being the upraise of the asthenosphere pumped from
 308 the deep mantle flow.

309 [19] **Acknowledgments.** Discussions with Enrico Bonatti, Roberto
 310 Sabadini and Giuliano Panza were invaluable. Jean-Yves Peterschmitt
 311 and Christophe Dumas provided technical help with ICE-5G data. Some
 312 figures were produced with the GMT software. Rob Sohn and an anony-
 313 mous referee are thanked for constructive revision. Research supported by
 314 Eurocores-CNR (TopoEurope-Topo4D project).

315 References

316 Asimow, P. D., and C. H. Langmuir (2003), The importance of water to
 317 oceanic mantle melting regimes, *Nature*, *421*, 815–820, doi:10.1038/
 318 nature01429.
 319 Bonath, E. (1990), Not so hot “hot spots” in the oceanic mantle, *Science*,
 320 *250*, 107–111, doi:10.1126/science.250.4977.107.
 321 Cathles, L. M. (1975), *The Viscosity of the Earth's Mantle*, 386 pp., Princeton
 322 Univ. Press, Princeton, N. J.
 323 Courtillot, V., A. Davaille, J. Besse, and J. Stock (2003), Three distinct
 324 types of hotspot in the Earth's mantle, *Earth Planet. Sci. Lett.*, *205*, 295–
 325 308, doi:10.1016/S0012-821X(02)01048-8.
 326 Doglioni, C., E. Carminati, and E. Bonatti (2003), Rift asymmetry and
 327 continental uplift, *Tectonics*, *22*(3), 1024, doi:10.1029/2002TC001459.
 328 Dziewonski, A. M., and D. L. Anderson (1981), Preliminary reference
 329 Earth model, *Phys. Earth Planet. Inter.*, *25*, 297–356, doi:10.1016/
 330 0031-9201(81)90046-7.
 331 Eldrett, J. S., I. C. Harding, P. A. Wilson, E. Butler, and A. P. Roberts
 332 (2007), Continental ice in Greenland during the Eocene and Oligocene,
 333 *Nature*, *446*, 176–179, doi:10.1038/nature05591.
 334 Foulger, G. R., and D. L. Anderson (2005), A cool model for the Iceland
 335 hotspot, *J. Volcanol. Geotherm. Res.*, *141*, 1–22, doi:10.1016/j.jvolgeores.
 336 2004.10.007.
 337 Foulger, G. R., et al. (2001), Seismic tomography shows that upwelling
 338 beneath Iceland is confined to the upper mantle, *Geophys. J. Int.*, *146*,
 339 504–530, doi:10.1046/j.0956-540x.2001.01470.x.

Gee, M. A. M., R. N. Taylor, M. F. Thirlwall, and B. J. Murton (1998), 340
 Glacioisostasy controls chemical and isotopic characteristics of tholeiites 341
 from the Reykjanes peninsula, SW Iceland, *Earth Planet. Sci. Lett.*, *164*, 342
 1–5, doi:10.1016/S0012-821X(98)00246-5. 343
 Gripp, A. E., and R. G. Gordon (2002), Young tracks of hotspots and 344
 current plate velocities, *Geophys. J. Int.*, *150*, 321–361, doi:10.1046/ 345
 j.1365-246X.2002.01627.x. 346
 Hardarson, B. S., J. G. Fitton, R. M. Ellam, and M. S. Pringle (1997), Rift 347
 relocation—A geochemical and geochronological investigation of a 348
 palaeo-rift in northwest Iceland, *Earth Planet. Sci. Lett.*, *153*, 181– 349
 196, doi:10.1016/S0012-821X(97)00145-3. 350
 Jull, M., and D. McKenzie (1996), The effect of deglaciation on mantle 351
 melting beneath Iceland, *J. Geophys. Res.*, *101*, 21,815–21,828, 352
 doi:10.1029/96JB01308. 353
 Kaban, M. K., O. G. Flóvenz, and G. Pálmason (2002), Nature of the crust- 354
 mantle transition zone and the thermal state of the upper mantle beneath 355
 Iceland from gravity modelling, *Geophys. J. Int.*, *149*, 281–299, 356
 doi:10.1046/j.1365-246X.2002.01622.x. 357
 Kaufmann, G., and K. Lambeck (2002), Glacial isostatic adjustment and the 358
 radial viscosity profile from inverse modeling, *J. Geophys. Res.*, *107*, 359
 2280, doi:10.1029/2001JB000941. 360
 Kitagawa, H., K. Kobayashi, A. Makishima, and E. Nakamura (2008), 361
 Multiple pulses of the mantle plume: Evidence from Tertiary Icelandic 362
 lavas, *J. Petrol.*, *49*, 1365–1396, doi:10.1093/ptrology/egm029. 363
 Langmuir, C. H., and D. H. Forsyth (2007), Mantle melting beneath mid- 364
 ocean ridges, *Oceanography*, *20*, 78–87. 365
 Lemoine, F. G., et al. (1998), The development of the joint NASA-GSFC 366
 and National Imagery and Mapping Agency (NIMA) geopotential model 367
 EGM96, *Tech. Pap. NASA/TP-1998-206861*, NASA Goddard Space 368
 Flight Cent., Greenbelt, Md. 369
 MacLennan, J., M. Jull, D. P. McKenzie, L. Slater, and K. Grönvold (2002), 370
 The link between volcanism and deglaciation in Iceland, *Geochem. Geophys. 371*
Geosyst., *3*(11), 1062, doi:10.1029/2001GC000282. 372
 McKenzie, D. P. (1984), The generation and compaction of partially molten 373
 rock, *J. Petrol.*, *25*, 713–765. 374
 Milne, G. A., J. L. Davis, J. X. Mitrovica, H.-G. Scherneck, J. M. Johansson, 375
 M. Vermeer, and H. Koivula (2001), Space-geodetic constraints on glacial 376
 isostatic adjustment in Fennoscandia, *Science*, *291*, 2381–2385, 377
 doi:10.1126/science.1057022. 378
 Mitrovica, J. X., and W. R. Peltier (1993), Constraints on mantle viscosity 379
 from relative sea level variations in Hudson Bay, *Geophys. J. Int.*, *19*, 380
 1185–1188. 381
 Montelli, R., G. Nolet, F. A. Dahlen, G. Masters, and R. E. Engdahl (2004), 382
 Finite-frequency tomography reveals a variety of plumes in the mantle, 383
Science, *303*, 338–343, doi:10.1126/science.1092485. 384
 Moran, K., et al. (2006), The Cenozoic palaeoenvironment of the Arctic 385
 Ocean, *Nature*, *441*, doi:10.1038/nature04800. 386
 Oxburgh, E. R., and E. M. Parmentier (1977), Compositional and density 387
 stratification in oceanic lithosphere; causes and consequences, *J. Geol. 388*
Soc., *133*(4), 343–355, doi:10.1144/gsjgs.133.4.0343. 389
 Peltier, W. R. (2004), Global glacial isostasy and the surface of the ice-age 390
 Earth: The ICE-5G (VM2) model and GRACE, *Annu. Rev. Earth Planet. 391*
Sci., *32*, 111–149, doi:10.1146/annurev.earth.32.082503.144359. 392
 Ramillien, G., A. Lombard, A. Cazenave, E. R. Ivins, M. Llubes, F. Remy, 393
 and R. Biancale (2006), Interannual variations of the mass balance of the 394
 Antarctica and Greenland ice sheets from GRACE, *Global Planet. 395*
Change, *53*, 198–208, doi:10.1016/j.gloplacha.2006.06.003. 396
 Ritsema, J., and R. M. Allen (2003), The elusive mantle plume, *Earth 397*
Planet. Sci. Lett., *207*, 1–12, doi:10.1016/S0012-821X(02)01093-2. 398
 Shillington, D. J., W. S. Holbrook, H. J. A. Van Avendonk, B. E. Tucholke, 399
 J. R. Hopper, K. E. Loudon, H. C. Larsen, and G. T. Nunes (2006), 400
 Evidence for asymmetric nonvolcanic rifting and slow incipient oceanic 401
 accretion from seismic reflection data on the Newfoundland margin, 402
J. Geophys. Res., *111*, B09402, doi:10.1029/2005JB003981. 403
 Sigvaldason, G. E. (2002), Volcanic and tectonic processes coinciding with 404
 glacialation and crustal rebound: An early Holocene rhyolitic eruption in 405
 the Dyngjufjöll volcanic centre and the formation of the Askja caldera, 406
 north Iceland, *Bull. Volcanol.*, *64*, 192–205, doi:10.1007/s00445-002- 407
 0204-7. 408
 Tapley, B. D., S. Bettadpur, J. Ries, P. F. Thompson, and M. M. Watkins 409
 (2004), GRACE measurements of mass variability in the Earth system, 410
Science, *305*(5683), 503–505, doi:10.1126/science.1099192. 411
 Tapley, B., et al. (2005), GGM02—An improved Earth gravity field model 412
 from GRACE, *J. Geod.*, *79*, 467–478, doi:10.1007/s00190-005-0480-z. 413
 Taylor, R. N., M. F. Thirlwall, B. J. Murton, D. R. Hilton, and M. A. M. Gee 414
 (1997), Isotopic constraints on the influence of the Icelandic plume, *Earth 415*
Planet. Sci. Lett., *148*, E1–E8, doi:10.1016/S0012-821X(97)00038-1. 416
 Turcotte, D. L., and G. Schubert (2002), *Geodynamics*, 456 pp., Cambridge 417
 Univ. Press, Cambridge, U. K. 418
 Vestøl, O. (2006), Determination of postglacial land uplift in Fennoscandia 419
 from leveling, tide-gauges and continuous GPS stations using least 420

- 421 squares collocation, *J. Geod.*, 80, 248–258, doi:10.1007/s00190-006-
422 0063-7. 425
- 423 Vink, G. E. (1984), A hotspot model for Iceland and the Voring plateau,
424 *J. Geophys. Res.*, 89, 9949–9959, doi:10.1029/JB089iB12p09949. 426
- Watts, A. B. (2001), *Isostasy and Flexure of the Lithosphere*, 472 pp.,
Cambridge Univ. Press, Cambridge, U. K. 428
- E. Carminati and C. Doglioni, Dipartimento di Scienze della Terra, 428
Università di Roma “La Sapienza,” P. le A. Moro 5, E-00185 Roma, Italy. 429
(eugenio.carminati@uniroma1.it) 430

Article in Proof